Vibrotactile Display of Patterned Surface Textures With Kinesthetic Haptic Devices Using Balanced Impulses

Ruisi Zhang, *Student Member, IEEE* and Jake J. Abbott, *Senior Member, IEEE*

***Abstract*—Kinesthetic haptic devices are designed primarily to display quasistatic and low-bandwidth forces and moments. Existing methods for vibrotactile display sometimes introduce haptic and/or audio artifacts. In this article, we propose a method to display vibrotactile stimulus signals of moderate to high frequency (20–500 Hz) using kinesthetic haptic devices with a standard 1 kHz haptic update rate. Our method combines symmetric square-wave signals whose periods are even multiples of the haptic update period with asymmetric square-wave signals whose periods are odd multiples of the haptic update period, while ensuring that the positive and negative impulses are balanced in both cases, and utilizing the just noticeable difference in frequency discrimination to avoid the need to display other frequencies. For frequencies at which the above method is insufficient, corresponding to a small band near 400 Hz for a 1 kHz update rate, we utilize a signal-mixing method. Our complete method is then extended to render haptic gratings by measuring scanning velocity, converting the local spatial frequency to its equivalent instantaneous temporal frequency, and displaying a single full-period vibration event. In a series of human-subject studies, we showed that our proposed method is preferred over existing methods for vibrotactile display of signals with relatively high-frequency content.**

***Index Terms*—High-frequency vibrations, asymmetric vibrations, vibration feedback, haptic gratings.**

I. Introduction

KINESTHETIC haptic devices are designed primarily to display quasistatic and low-bandwidth forces and moments. Kinesthetic devices are typically driven by one or more back-drivable DC motors, controlled at a native servo loop rate of 1 kHz [1]. Vibrotactile display is important for event-based feedback [2], [3], rendering haptic textures [4]–[6], and even musical haptics [7]. However, kinesthetic haptic devices are not optimized for vibrotactile display over the entire frequency range (20–1000 Hz [8], [9]) that humans are able to detect.

Manuscript received February 25, 2020; revised September 3, 2020 and March 15, 2021; accepted April 8, 2021. Date of publication April 12, 2021; date of current version December 16, 2021. This work was supported by the National Science Foundation under grant number 1423273. This article was recommended for publication by Associate Editor Dr. Y. Tanaka and Editor-in-Chief Prof. D. Prattichizzo upon evaluation of the reviewers' comments. *(Corresponding author: Ruisi Zhang.)*

The authors are with the Department of Mechanical Engineering and the Robotics Center, University of Utah, Salt Lake City, UT 84112 USA (e-mail: Ruisi.Zhang@utah.edu; jake.abbott@utah.edu).

Digital Object Identifier 10.1109/TOH.2021.3072588

Many engineered surfaces that we may wish to render in virtual environments have regular patterns (Fig. 1), so they are of particular interest. Patterned surface textures are described by a small number of spatial frequencies, which result in temporal frequencies proportional to the scanning velocity of the user. The preferred update rate for the rendering of haptic textures is 5–10 kHz [10], which is an order of magnitude faster than typical kinesthetic devices. There are two principal approaches to improve a kinesthetic haptic device's ability to render patterned textures. One is to attach auxiliary vibrotactile actuators (some of which are commercially available) that are well suited to the frequency ranges of interest [6], [11], [12]. The other is to make improvements to the techniques that use the device's native actuators and 1 kHz control software [2], [13], [14]; this is our focus.

Culbertson *et al.* [6], [14] suggested that data-driven haptic texture models that were originally rendered at a rate of 10 kHz can also be applied to kinesthetic devices using downsampled models. This represents the state of the art in the use of kinesthetic devices to display stochastic isotropic textures in which the description of the local texture properties is invariant to position (e.g., sandpaper, cinder block). However, this method seems to be not ideal for patterned surface textures (e.g., gratings) with a known geometric model, as the stochastic methods introduce a feeling and sound that is best described as noisy or gritty, which is not present when interacting with real patterned surface textures.

Patterned surface textures are often modeled as a geometry-based height map and rendered on haptic devices run at higher update rate of 2–10 kHz [5], [15]–[18]. For complicated patterned surface textures, Shin and Choi [15] suggested to create the height map using photometric stereo to capture the microgeometry of a textured surface. For simple patterned surface textures, the height map for triangular, square-wave, and sinusoidal gratings are modeled by reconstructing the corresponding vibration signals [5], [19]–[21]. We are particularly interested in rendering square-wave gratings because they are relatively simple to implement and can reach the highest temporal frequencies (i.e., 500 Hz square-wave with a 1 kHz haptic update rate).

Humans are not sensitive to the difference between square-wave gratings and sinusoidal gratings based on their waveform, especially at high frequencies [22]. Cholewiak *et al.* [5] found that humans cannot distinguish square-wave gratings

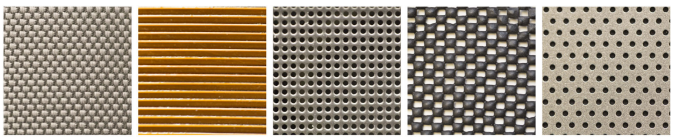

Fig. 1. Examples of patterned surface textures (from left to right): Nylon, electromagnetic coil, speaker surface, rubber mesh, and pegboard.

from sinusoidal gratings of the same spatial period (i.e., wavelength) up to 6.4 mm (i.e., spatial frequency greater than 0.16 mm $^{-1}$) and an amplitude (i.e., half peak to peak) that is approximated by the coefficient of the fundamental component in the Fourier expansion. These findings suggest that we can use square-wave gratings to create the vibrotactile illusion of sinusoidal gratings. For a square wave of amplitude A, the Fourier-expansion method results in an equivalent sinusoid with amplitude $A_F = (4/\pi)A$. Although this finding was stated in terms of spatial frequency f_s (units m^{-1}), it can be restated in terms of temporal frequency $f_t = f_s v$ (units Hz) by considering a constant scanning velocity v (units m$\cdot$ s^{-1}); this is an equivalence relationship that we will use throughout this paper. Landin *et al.* [23] suggested the total energy spectral density (ESD) should be preserved in the transformation of human vibrotactile sensations. This energy-preserving method results in a sinusoid with amplitude $A_E = (\sqrt{2})A$. These two equivalence relationships between sinusoids and square waves are similar but not identical.

We are interested in displaying temporal square-wave vibrations throughout the frequency range of 20–500 Hz using a kinesthetic haptic device with an update rate of 1 kHz. If the vibration signal to be generated happens to have a period that is an even multiple of the haptic update period (which we will refer to as an even-period signal), we can perfectly display the square-wave signal using the zero-order hold (ZOH) with equal time (i.e., an equal number of haptic updates) being split between A and $-A$. However, it is less clear how to handle signals at other frequencies (i.e., other temporal periods), where perceived artifacts are introduced due to aliasing.

Prior studies [24]–[27] have described the dissimilarities of vibrotactile sensations between simple sinusoidal vibrations and vibrations that are constructed by superimposing two or more sinusoidal vibrations with distinct frequencies. Friesen *et al.* [18] recently found that the human hand perceives a multi-frequency grating as an equivalent single-frequency grating, albeit for a higher frequency range than we consider here, and they suggested a formula to characterize the mapping. We initially hypothesized that this method could be extended for use in the display of signals of arbitrary frequency as some combination of two even-period signals, which can each be perfectly displayed as described above. However, we will show that, although this approach can be useful in a limited context, it causes some undesirable perceived artifacts, especially at low frequencies.

In this paper, we propose a method to display vibrotactile stimulus signals of moderate to high frequency (20–500 Hz) using kinesthetic haptic devices with a standard 1 kHz haptic update rate. Our method combines symmetric square-wave signals whose periods are even multiples of the haptic update period with asymmetric square-wave signals whose periods are odd multiples of the haptic update period, while ensuring that the positive and negative impulses are balanced in both cases, and utilizing the just noticeable difference (JND) in frequency discrimination to avoid the need to display most other frequencies. For frequencies at which the balanced-impulse method is insufficient, corresponding to a small band near 400 Hz for a 1 kHz update rate, we utilize a weighted mixing method inspired by [18]. Our method is then extended to render haptic gratings by measuring scanning velocity, converting the local spatial frequency to its equivalent temporal frequency, and displaying a single full-period vibration event. We conduct a series of human-subject studies to evaluate our proposed method by comparing it to existing methods [5].

We note that, unlike prior works that have used asymmetric vibrations to intentionally display a perceived net force when using vibrotactile actuators [28]–[32], here we use asymmetric vibrations to explicitly avoid an actual net force when implementing vibrotactile display with a grounded kinesthetic haptic device.

II. Temporal Vibrations

This section describes three potential methods to display open-loop temporal square-wave vibrations (which we will refer to as Methods T1–T3) throughout the frequency range of 20–500 Hz using a kinesthetic haptic device with DAC ZOH and a standard haptic update rate of $f_h = 1$ kHz (i.e., update period $T_h = 0.001$ s). We utilize these methods to reconstruct discrete-time square-wave signals using the discrete-time index k that is updated at f_h for a desired symmetric square-wave vibration with temporal frequency f_t (i.e., temporal period $T = 1/f_t$) and amplitude A (where any conversion from the amplitude of some desired sinusoidal signal has already occurred). Based on the control mode of the vibratactile display, A may denote position [32], force or moment at the end-effector [31], (generalized) torque at the joint level [28], or commanded current used in a voice-coil actuator [29], [30]. Throughout this paper, we will use the terms "even-period" and "odd-period" to represent temporal periods that are even and odd multiples of the haptic update period, respectively (i.e., $T = 0.001z$ for some integer z). All three methods are capable of perfectly displaying even-period vibrations. The differences between methods are observed when we consider signals with other temporal periods (Fig. 2).

A. Method T1 (Sampling a Continuous Function)

Method T1 displays a square-wave vibration signal $V_{\mathrm{T1}}[k]$ using Algorithm 1. The basic idea is to obtain a temporal period that approximates the desired period, and to divide that temporal period into positive and negative portions of equal magnitude and approximately equal duration. We note that this method is equivalent to a purely temporal version of the spatiotemporal haptic-grating method of [5], which is described as Method S1 in Section III-A, if the user adopts a constant scanning velocity.

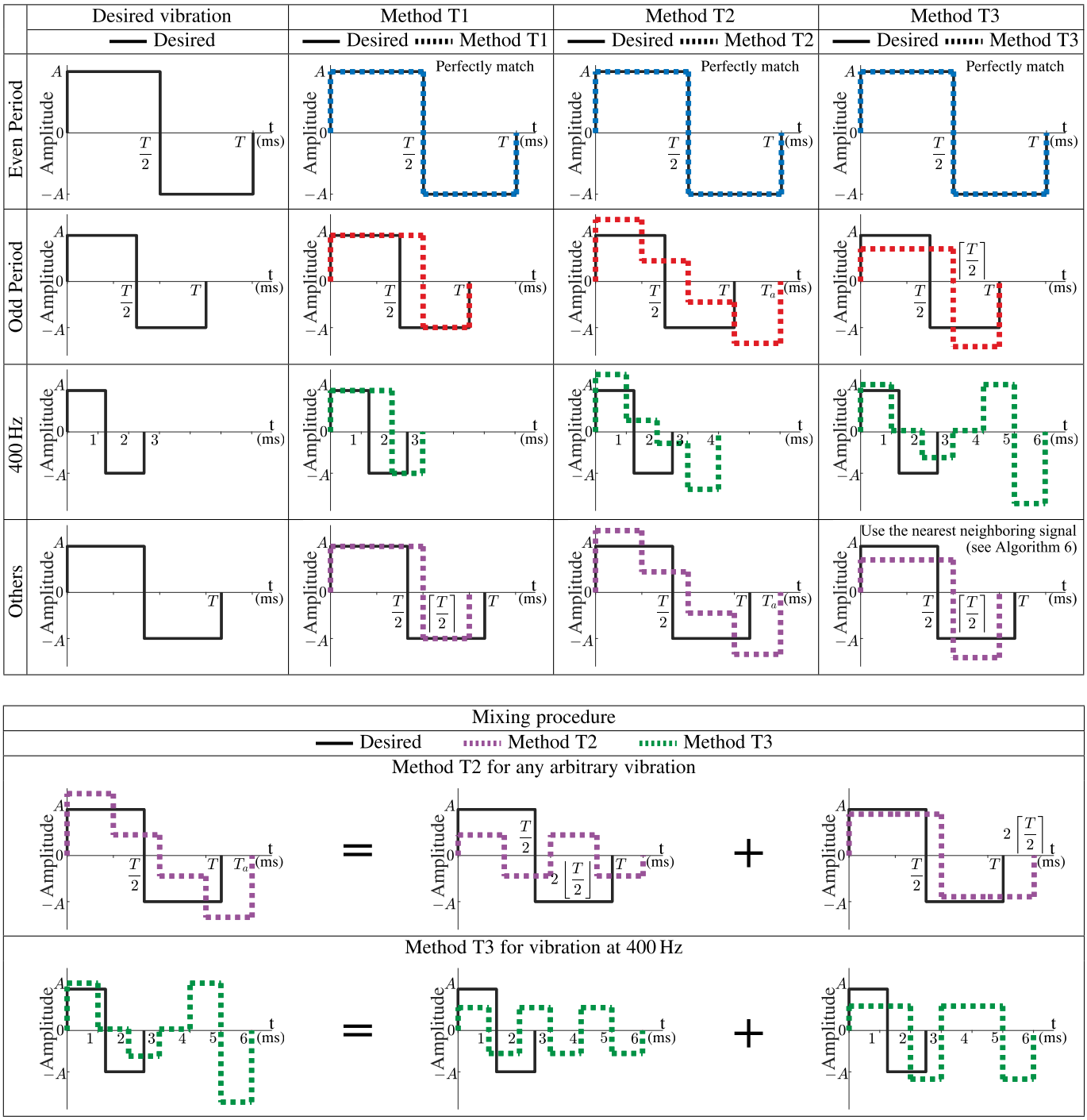

Fig. 2. (Upper) Comparison of three candidate temporal methods used to display a full-cycle desired square-wave vibration with even-period, odd-period, 400 Hz (which is handled as a special case in Method T3), and all other frequencies. Note, vibrations with even-period, odd-period, and 400 Hz here correspond to those in Fig. 3. (Lower) Mixing procedure with no phase shifting. Method T2 displays any desired vibration by mixing two neighboring even-period vibration components with $T = 0.002\lceil \frac{T}{0.002} \rceil$ and $T = 0.002\lfloor \frac{T}{0.002} \rfloor$, leading to a vibration with actual temporal period T_a. Method T3 only needs to display the desired vibration at 400 Hz by mixing the neighboring even-period ($T = 0.002$ s) and odd-period ($T = 0.003$ s) vibration components, leading to the vibration with $T_a = 0.006$ s. Note, T_a is the least common multiple of the two Ts of the vibration components.

As can be seen in Fig. 2, this method often results in signals that spend more time at A than at $-A$ when a vibration signal starts with A, and vice versa. This leads to a net force in one direction, and also induces higher-order frequency components. We find that these undesirable artifacts are particularly salient at relatively high frequencies.

B. *Method T2 (Weighted Mixing)*

Since it is possible to perfectly display even-period vibrations with a kinesthetic device, the basic idea of Method T2 is to display a vibration at any given period that is not even-period by mixing the two neighboring even-period vibrations (i.e., the one below and the one above). Each of

Algorithm 1. Temporal vibration using Method T1

Input: Temporal period T, amplitude A, discrete-time index k

procedure $V_{\mathrm{T1}}[k]$
  $N \leftarrow \frac{T}{T_h}$ ▷N: number of haptic updates in a cycle
  $\theta \leftarrow (k \text{ modulo } N)$ ▷θ: current position in a cycle
  if $\theta < \frac{N}{2}$ **then** ▷1st part of the cycle
    $V_{\mathrm{T1}}[k] \leftarrow A$ ▷positive pulse
  else ▷2nd part of the cycle
    $V_{\mathrm{T1}}[k] \leftarrow -A$ ▷negative pulse
  end if
end procedure

Algorithm 2. Even-period vibration for use in Methods T2 and T3

Input: Temporal period T, amplitude A, discrete-time index k

procedure $V_{\mathrm{even}}[k]$
  $N \leftarrow \mathrm{round}(\frac{T}{T_h})$ ▷N: number of haptic updates in a cycle
  $\theta \leftarrow (k \text{ modulo } N)$ ▷θ: current position in a cycle
  if $\theta < \frac{N}{2}$ **then** ▷1st half of the cycle ($\frac{N}{2}$ haptic updates)
    $V_{\mathrm{even}}[k] \leftarrow A$ ▷positive pulse
  else ▷2nd half of the cycle ($\frac{N}{2}$ haptic updates)
    $V_{\mathrm{even}}[k] \leftarrow -A$ ▷negative pulse
  end if
end procedure

these two even-period vibrations can be generated using Algorithm 2.

We use an inverse of a method proposed by Friesen *et al.* [18] to mix the two neighboring even-period vibrations (Lower figure in Fig. 2). They found that a haptic grating with two spatial-frequency components f_{s1} and f_{s2}, of respective amplitudes A_1 and A_2, could be approximated as a haptic grating with a single spatial frequency $f_s = (A_1 f_{s1} + A_2 f_{s2})/(A_1 + A_2)$. Although this result was stated in terms of spatial frequency, it can be restated in terms of temporal frequency by considering a constant scanning velocity v, as described earlier. After appropriate substitutions, the perceived period T can be estimated by

$$\frac{1}{T} = \frac{\frac{A_1}{T_1} + \frac{A_2}{T_2}}{A_1 + A_2}. \tag{1}$$

where the temporal periods of the two neighboring even-period vibrations are T_1 for the one below T and T_2 for the one above T. We are interested in the inverse of this problem: Given a desired vibration signal with temporal frequency f_t (i.e., period T) and amplitude A, what are the amplitudes A_1 and A_2 of the two neighboring even-period signals that will result in a perceived amplitude of A?

If the total ESD is preserved in the transformation of human perception of high-frequency vibrations as suggested in [23], [42], then the ESD of the desired vibration should be the same as the total ESD of the two even-period vibration components during the mixing procedure. The ESD of a discrete-time signal $x_k = x(kT_h)$ can be calculated by $\mathrm{ESD} = T_h^2 \sum_{k=-\infty}^{\infty} (x_k e^{-2\pi k i})^2$, where T_h is the haptic update period and i is the imaginary unit. The ESD of a standard square waveform can be calculated by $\mathrm{ESD} = A^2$. The energy equivalency between the desired vibration and the two even-period vibration components is

$$A^2 = A_1^2 + A_2^2. \tag{2}$$

We use (1) and (2) to solve for the amplitudes A_1 and A_2:

$$A_1 = A\sqrt{\frac{T_1^2T_2^2 - 2TT_1^2T_2 + T^2T_1^2}{2T_1^2T_2^2 - 2TT_1^2T_2 - 2TT_1T_2^2 + T^2T_1^2 + T^2T_2^2}} \tag{3}$$

$$A_2 = A\sqrt{\frac{T_1^2T_2^2 - 2TT_1T_2^2 + T^2T_2^2}{2T_1^2T_2^2 - 2TT_1^2T_2 - 2TT_1T_2^2 + T^2T_1^2 + T^2T_2^2}} \tag{4}$$

We consider the two vibration components are perfectly in phase to simplify the mixing procedure, since the phase information between frequency components is perceptually irrelevant [5], [17]. Finally, the mixed vibration signal $V_{\mathrm{T2}}[k]$ is constructed using Algorithm 3.

Algorithm 3. Temporal vibration using Method T2

Input: Temporal period T, amplitude A, discrete-time index k

procedure $V_{\mathrm{T2}}[k]$
  $T_1 = 2T_h\lceil T/(2T_h)\rceil$ ▷use ceiling function
  $T_2 = 2T_h\lfloor T/(2T_h)\rfloor$ ▷use floor function
  $A_1, A_2 \leftarrow$ Equations (3) and (4)
  $V_{\mathrm{even},1}[k] \leftarrow$ Algorithm 2 given T_1, A_1, k
  $V_{\mathrm{even},2}[k] \leftarrow$ Algorithm 2 given T_2, A_2, k
  $V_{\mathrm{T2}}[k] \leftarrow V_{\mathrm{even},1}[k] + V_{\mathrm{even},2}[k]$
end procedure

As can be seen in Fig. 2, this method generates signals that often include higher-order frequency components. This creates artifacts that can sometimes be felt and/or heard. We find these artifacts are particularly salient at relatively low frequencies.

C. Method T3 (Proposed Balanced-Impulse Method)

Although it is difficult to display vibrations at any given temporal frequency in the frequency range of 20–500 Hz, we have already seen that we can perfectly display even-period vibrations. In addition, we have developed a method to display odd-period vibrations with high haptic and audio fidelity (Section II-C2). The basic idea of Method T3 to handle most other temporal frequencies is to capitalize on the JND in frequency discrimination and approximate any other desired temporal frequency by its nearest even-period or odd-period neighbor, with the observation that both neighbors are within the JND of each other throughout most of our frequency range of interest, with the only exception being the transition between 333 Hz and 500 Hz (see Fig. 3). Method T3 includes a special case (Section II-C3) to address this small range.

Young *et al.* [35] showed that the audio-plus-haptic JND is only slightly smaller than the audio-only JND around their selected reference frequency of 160 Hz, which suggested that audio signals are likely dominating the perception of subjects when both audio and haptic signals are present. Throughout

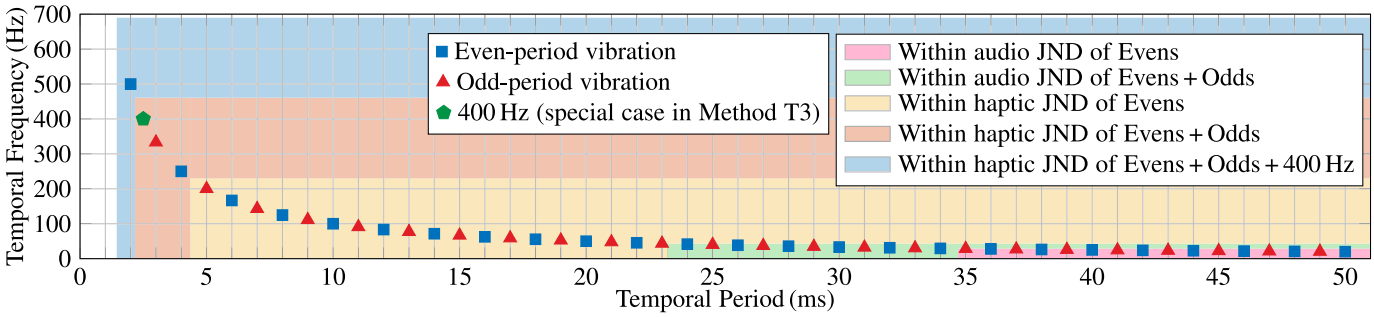

Fig. 3. Temporal periods T in the range 0.002–0.050 s, with their corresponding temporal frequencies $f_t = 1/T$ in the range 20–500 Hz, that are considered in Method T3, which include even and odd multiples of the haptic update period 0.001 s, as well as a special case of $f_t = 400$ Hz. The different colored regions indicate where the difference in f_t between any given vibration and its nearest achievable neighboring vibrations is within the audio or haptic just noticeable difference (JND), which are reported in [33]–[35]. We estimated the haptic JND at a temporal frequency that is not directly reported in prior works by the average frequency discrimination Weber fractions $\mathrm{WF} = \mathrm{JND}/f_t \approx 0.38$ for all conditions in [34], which is also close to the midpoint ($\mathrm{WF} = 0.37$) of the range $\mathrm{WF} = 0.020$–0.72 throughout the frequency range of 20–512 Hz reported in [33], [36]–[41].

this paper, including our depiction of the two colored "audio" boxes in Fig. 3, we assume that audio feedback dominates haptic feedback whenever audio feedback is present.

1) Even-Period Signals: For even-period signals, we use Algorithm 2. If we consider using only even-period vibrations, Fig. 3 shows that we can display signals throughout the frequency range of 20–230 Hz without any perceivable haptic discretization. We will still be able to hear the discretization for frequencies above 28.8 Hz. However, even if we limit ourselves to consideration of only haptic effects, this still falls well short of the full 20–500 Hz frequency range of interest.

2) Odd-Period Signals: Although odd-period vibrations cannot be perfectly reconstructed as symmetric square-wave signals, they can be approximated by (i.e., be perceptually similar to) asymmetric square-wave signals with the correct temporal period using Algorithm 4 (see Fig. 2). We are interested in the following problem: Given a desired odd-period vibration signal with temporal frequency f_t (period T) and amplitude A, what are the magnitudes A_p for the positive pulse with duration T_p and A_n for the negative pulse with duration T_n that will result in a perceived amplitude of A? We consider two constraints to solve for the two unknowns A_p and A_n. The first constraint is that the positive impulse (i.e., the product of magnitude and time) should equal the negative impulse to avoid any net force in one direction:

$$A_p T_p = A_n T_n. \tag{5}$$

The second constraint is that the ESD of this asymmetric square-wave signal should equal the ESD of the desired odd-period vibration signal:

$$\frac{A_p^2 T_p + A_n^2 T_n}{T} = A^2. \tag{6}$$

We use (5) and (6) to solve for the amplitudes A_p and A_n:

$$A_p = A\sqrt{\frac{TT_n}{T_p^2 + T_n T_p}}, \qquad A_n = A\sqrt{\frac{TT_p}{T_n^2 + T_n T_p}}. \tag{7}$$

Algorithm 4. Odd-period vibration for use in Method T3

Input: Temporal period T, amplitude A, discrete-time index k

procedure $V_{\mathrm{odd}}[k]$
  $T_p = T_h\lceil T/(2T_h)\rceil$ ▷use ceiling function
  $T_n = T_h\lfloor T/(2T_h)\rfloor$ ▷use floor function
  $A_p, A_n \leftarrow$ Equation (7)
  $N \leftarrow \mathrm{round}(\frac{T}{T_h})$ ▷N: number of haptic updates in a cycle
  $\theta \leftarrow (k \bmod N)$ ▷θ: current position in a cycle
  if $\theta < \frac{N}{2}$ **then** ▷1st part of the cycle ($\frac{N+1}{2}$ haptic updates)
    $V_{\mathrm{odd}}[k] \leftarrow A_p$ ▷positive pulse
  else ▷2nd part of the cycle ($\frac{N-1}{2}$ haptic updates)
    $V_{\mathrm{odd}}[k] \leftarrow -A_n$ ▷negative pulse
  end if
end procedure

We note that the odd-period signals rendered by Method T3 are the same as those rendered by Method T1 but shifted by an appropriate amount to avoid rendering a net force.

If we consider using both even-period and odd-period vibrations, Fig. 3 shows that we can now display signals throughout the entire frequency range of 20–461 Hz without any perceivable haptic discretization. We will still be able to hear the discretization for frequencies above 43.1 Hz. These values are both improvements from only considering even-period vibrations. However, the transition from 461 Hz to 500 Hz is still perceived as haptically discontinuous, which we would like to remedy.

3) Special Case of 400 Hz: To provide a smooth haptic transition from 333 Hz to 500 Hz, we introduce the approximated vibration at 400 Hz ($T = 0.0025$ s) by mixing the two neighboring vibration signals, in phase, at 500 Hz ($T = 0.002$ s) and 333 Hz ($T = 0.003$ s), using Algorithm 5, which is similar to Method T2. We chose the special case to be at 400 Hz (as opposed to some other frequency in the 333–500 Hz range) for two reasons. First, it has a temporal period (0.0025 s) that is at the midpoint of the nearest neighbors (0.002 s and 0.003 s), which enables the entire vibration event to be completed in 0.006 s (see Fig. 2). Second, if we consider the individual JND regions for 333 Hz and for 500 Hz, we find

Algorithm 5. 400 Hz vibration for use in Method T3

Input: Amplitude A, discrete-time index k

procedure $V_{400}[k]$
  $A_{\text{even}}, A_{\text{odd}} \leftarrow$ Equation (8)
  $V_{\text{even}}[k] \leftarrow$ Algorithm 2 given $T_{\text{even}} = 2T_h$, A_{even}, k
  $V_{\text{odd}}[k] \leftarrow$ Algorithm 4 given $T_{\text{odd}} = 3T_h$, A_{odd}, k
  $V_{400}[k] \leftarrow V_{\text{even}}[k] + V_{\text{odd}}[k]$
end procedure

Algorithm 6. Temporal vibration using Method T3

Input: Temporal period T, amplitude A, discrete-time index k

procedure $V_{\text{T3}}[k], T_a$ ▷T_a: actual temporal period
  if $T < 2.25T_h$ **then** ▷highest temporal frequency of $\frac{1}{2T_h}$
    $T_a \leftarrow 2T_h$
    $V_{\text{T3}}[k] \leftarrow$ Algorithm 2 given T_a, A, k
  else if $T \leq 2.75T_h$ **then** ▷special case of 400 Hz
    $T_a \leftarrow 6T_h$ ▷common multiple of $2T_h$ and $3T_h$
    $V_{\text{T3}}[k] \leftarrow$ Algorithm 5 given A, k
  else
    $T_a \leftarrow \text{round}(\frac{T}{T_h})T_h$
    if $(\frac{T_a}{T_h}$ modulo $2) = 0$ **then** ▷even-period
      $V_{\text{T3}}[k] \leftarrow$ Algorithm 2 given T_a, A, k
    else ▷odd-period
      $V_{\text{T3}}[k] \leftarrow$ Algorithm 4 given T_a, A, k
    end if
  end if
end procedure

that 400 Hz is approximately equally far from the extremes of both of those regions.

We are interested in the following problem: Given a desired square-wave signal with temporal frequency 400 Hz and amplitude A, what are the amplitudes A_{even} and A_{odd} of the two neighboring vibration signals that will result in perceived amplitude of A? To solve for these amplitudes, we use (1) and (2), given the desired temporal frequency $f_t = 400$ Hz ($T = 0.0025$ s) and amplitude A, which results in

$$A_{\text{even}} = \left(\frac{2}{\sqrt{13}}\right)A, \qquad A_{\text{odd}} = \left(\frac{3}{\sqrt{13}}\right)A. \tag{8}$$

If we consider using this spacial case of 400 Hz along with both even-period and odd-period vibrations, Fig. 3 shows that we can now display signals through the entire desired frequency range of 20–500 Hz without any perceivable haptic discretization. However, we will still be able to hear the discretization for frequencies above 41.7 Hz, which may be inevitable with the relatively low haptic update rate of 1000 Hz.

4) Nearest Neighbor: In the preceding, we have described methods to display vibrations whose temporal periods are integer multiples of the haptic update period $T_h = 0.001$ s, as well as vibrations with a temporal frequency of $f_t = 400$ Hz ($T = 0.0025$ s). The final step in Method T3 is to take any given desired vibration and determine its nearest neighbor to display. This process is provided as Algorithm 6.

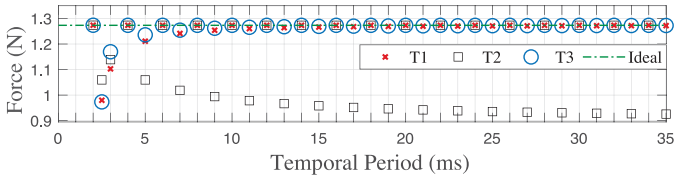

(a) Fundamental component

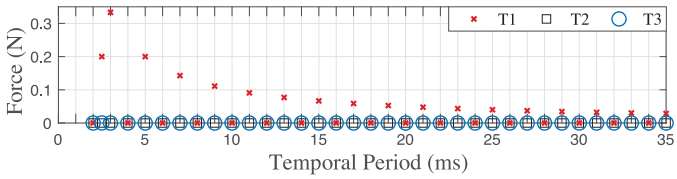

(b) Net force

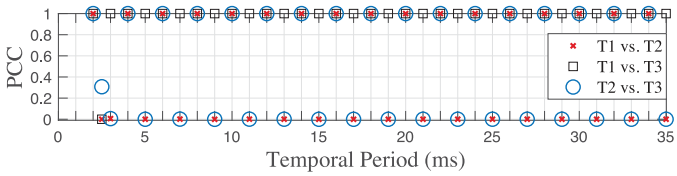

(c) Pearson correlation coefficient (PCC)

Fig. 4. Comparisons of three candidate temporal methods, using the force signals rendered by each of the three methods, across temporal periods T in the range 0.002–0.035 s, corresponding to a desired intensity of $A = 1$ N, which has an ideal fundamental component of 1.27 N, and a desired net force of 0 N. All signals are rendered at 1 kHz and then sampled at 40 kHz to approximate a 1 kHz sample-and-hold. (a) Fundamental component. (b) Net force, (c) Pearson correlation coefficient (PCC).

D. Comparison of Three Candidate Temporal Methods

This section quantitatively compares the vibration signals rendered using each of the three candidate temporal methods (i.e., Methods T1–T3) to display even-period and odd-period signals throughout the frequency range of interest, as well at 400 Hz (i.e., temporal period of 2.5 ms). All signals have a desired square-wave intensity of $A = 1$ N. Each signal is run for 40 complete periods, updated with a 1-kHz update rate, but then sampled at a 40-kHz sampling rate to approximate a near-ideal D/A sample-and-hold operation.

1) Fundamental Component: We begin by comparing the fundamental components of the signals generated by the three candidate temporal methods, since it has been shown that humans are most sensitive to the fundamental component [5]. Fig 4(a) shows the amplitude and the temporal period of the fundamental components of the force signals. These values were obtained by computing the discrete Fourier transform of the signals using the fast Fourier transform (fft) function in MATLAB. Note that the commanded square-wave signal of intensity $A = 1$ N has an ideal fundamental component of $4\ A/\pi = 1.27$ N. For even-period signals, the fundamental components for all three methods are equal to the ideal fundamental component. The other signals rendered using T1 and T3 have similar fundamental components at all temporal periods, with small differences observed for signals with relatively high frequency (i.e., relatively small temporal periods), which implies these two methods will provide a similar perceived

amplitude. At these same relatively high frequencies, both T1 and T3 have fundamental components with amplitudes that are lower than the ideal fundamental component. This is true of Method T2 across the entire range of frequencies. Only at 400 Hz (i.e., temporal period of 2.5 ms) does Method T2 get closer to the ideal than both other methods.

2) Net Force: Next, we characterize the net force (i.e., average force) of the signals generated by the three candidate temporal methods (Fig. 4(b)). In all cases, there is no desired net force, so any net force should be viewed as parasitic. Fig 4 (b) shows the average force of full-cycle commanded force signals that can be used for the haptic device with 1 kHz update rate. Both Methods T2 and T3 have no net force for all signals; neither does Method T1 for even-period signals. However, Method T1 shows a substantial net force (as much as 1/3 of the commanded vibration intensity) at relatively high frequencies (i.e., relatively small temporal periods).

3) Correlation Coefficient: Finally, we performed pairwise comparisons between the signals rendered using the three candidate temporal methods using the Pearson correlation coefficient (PCC), $\rho_{A,B} = \mathrm{cov}(A, B)/(\sigma_A \sigma_B)$, where cov is the covariance of the two variables A and B, and σ_i is the standard deviation of variable i. The PCC is influenced by differences in the fundamental components as well as components at higher frequency, but it is not influenced by any differences in net force. Fig 4(c) shows the PCC for each pairwise comparison. The PCC values for the signals from Methods T1 and T3 are identical at all frequencies except 400 Hz (i.e., 2.5 ms), meaning that they feel approximately identical in terms of frequency content. Method T2 also feels the same for even-period signals, but for odd-period signals, as well as 400 Hz, there are substantial differences from the other two methods; Methods T2 and T3 are more similar at 400 Hz than are either T1 and T3 or T1 and T2.

4) Discussion: Based on Fig. 4, we expect Methods T1 and T3 to be very similar to each other in terms of perceived amplitude and frequency content across the entire frequency range of interest. However, Method T1 has a parasitic net force at relatively high frequencies, which is not present in Method T3. We expect Method T2 to have fundamental-component amplitudes that are discontinuous when transitioning between neighboring frequencies, across the entire frequency range of interest. We also anticipate that Method T2 will feel substantially different from Methods T1 and T3 for odd-period signals.

III. Spatiotemporal Haptic Gratings

This section describes two potential methods to render virtual haptic square-wave gratings (which we will refer to as Methods S1 and S2) using a kinesthetic haptic device with DAC ZOH and a standard haptic update rate of $f_h = 1$ kHz (i.e., update period $T_h = 0.001$ s). Without loss of generality, we consider the haptic grating as a 2D virtual environment (Fig. 5) parameterized by a spatial period $\lambda = 1/f_s$ (units m) and amplitude A (units m). In a 2D virtual environment, the position of the haptic interaction point (HIP) in denoted by

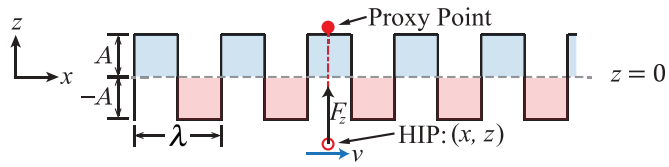

Fig. 5. Square-wave haptic grating in a 2D virtual environment.

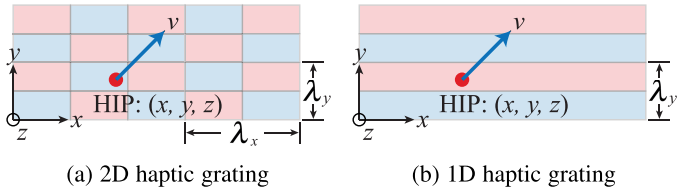

Fig. 6. Top-view of square-wave haptic grating in a 3D virtual environment. (a) 2D haptic grating with spatial periods λ_x and λ_y). (b) 1D haptic grating with spatial period λ_y. Note: the blue area has height $z = A$ and the pink area has height $z = -A$. (a) 2D haptic grating. (b) 1D haptic grating.

coordinates (x, z) in a coordinate system in which the x axis is along the surface and the z axis is normal to the surface; $\mathbf{v} = [\dot{x}\ 0]^\top$ is the instantaneous scanning velocity. In a 3D virtual environment (Fig. 6), the position of the HIP is denoted by coordinates (x, y, z) in a coordinate system in which the x–y plane is the surface plane and the z axis is normal to the surface; $\mathbf{v} = [\dot{x}\ \dot{y}\ 0]^\top = [v_x\ v_y\ 0]^\top$ is the instantaneous scanning velocity. The normal force F_z to render a surface with a haptic grating is

$$F_z = \begin{cases} K(H - z) & \text{if } z < H \\ 0 & \text{if } z \geq H. \end{cases} \tag{9}$$

where K (units $\mathrm{N} \cdot \mathrm{m}^{-1}$) is the stiffness of the virtual environment. The difference between Methods S1 and S2 is how we calculate and implement the height map H.

A. Method S1 (Sampling a Continuous Function)

Cholewiak *et al.* [5] developed a widely used rendering method to define the height map H_{S1} for haptic square-wave gratings in 2D virtual environments based on the grating's geometric parameters and the HIP's current position:

$$H_{\mathrm{S1,2D}} = \begin{cases} A & \text{if } \sin(2\pi x/\lambda) \geq 0 \\ -A & \text{if } \sin(2\pi x/\lambda) < 0. \end{cases} \tag{10}$$

If a constant scanning velocity $\mathbf{v}$ is used, this method will display a vibration that is identical to Method T1 with $T = \lambda/||\mathbf{v}||$. Prior studies [4], [10] found that Method S1 using kinesthetic devices with an update rate of 1 kHz (which is well below the preferred update rate of 5–10 kHz) for the rendering of sinusoidal haptic gratings, especially for fine gratings, might cause the unrealistic sensation of "buzzing" that was described as "high-frequency vibratory noise embedded in low-frequency vibrations". It is reasonable to assume that similar undesirable artifacts may exist when rendering square-wave haptic gratings.

To apply this method on surfaces in 3D virtual environments, we can associate a coordinate frame with surface with the z axis as the surface normal (without loss of generalization), and then characterize the spatial frequencies in each of the x and y directions by $f_{sx} = 1/\lambda_x$ and $f_{sy} = 1/\lambda_y$ (see Fig. 6). Note that we use spatial frequencies here, as opposed to spatial periods, since the spatial period may be undefined (i.e., infinite) in certain cases (see Fig. 6(b)). We then extend this method to define the height map $H_{S1,3D}$ for haptic square-wave gratings in 3D virtual environments based on the grating's geometric parameters and the HIP's current position:

$$H_{\mathrm{S1,3D}} = \begin{cases} A & \text{if } \cos(2\pi f_{sx} x)\cos(2\pi f_{sy} y) \geq 0 \\ -A & \text{if } \cos(2\pi f_{sx} x)\cos(2\pi f_{sy} y) < 0. \end{cases} \quad (11)$$

B. Method S2 (Proposed Balanced-Impulse Method)

Our proposed Method S2 is the spatiotemporal equivalent of Method T3. Unlike standard haptic-grating methods that use spatial frequency content [5], [18], [43], Method S2 uses the scanning velocity $\mathbf{v}$ to convert the local spatial-frequency content into a corresponding temporal frequency as $f_t = f_s||\mathbf{v}||$, which is more in line with how stochastic textures are typically displayed [6], [14], [44]. A single temporal vibration event (i.e., a full period of vibration) is then calculated using Method T3, given $T = 1/f_t$ and A. This vibration is calculated in terms of height (as opposed to force, for example), so that it can be incorporated directly into (9). Then, we only request a new vibration event (i.e., update T and A in Method T3) once a single full-period vibration event has completed. The complete algorithm to calculate the height map H_{S2} is provided in Algorithm 7.

To apply this method on surfaces in 3D virtual environments, the instantaneous spatial frequency can be approximated as

$$f_s = \begin{cases} f_{sx}\cos(\theta) & \text{if } \theta \leq \operatorname{atan2}(f_{sx}, f_{sy}) \\ f_{sy}\sin(\theta) & \text{if } \theta > \operatorname{atan2}(f_{sx}, f_{sy}) \end{cases} \quad (12)$$

where

$$\theta = \operatorname{atan2}(|v_y|, |v_x|) \quad (13)$$

Note that this formulation results in the perfect spatial frequency when moving in either the x or y direction, as well as when moving in the corner-to-corner diagonal direction for rectangular grids (e.g., Fig. 6(a)), and varies continuously between those cases.

Algorithm 7. Full-period vibration event using Method S2

Input: Spatial frequency f_s, amplitude A, scanning speed $\|\mathbf{v}\|$, vibration-event index j (global variable initialized at $j = 0$), actual temporal period T_a (global variable initialized at $T_a = 0$)

procedure H_{S2}, j, T_a
  if $j = 0$ **then** ▷no ongoing vibration event
    if $||\mathbf{v}|| < 0.001$ **or** $f_s = 0$ **then** ▷no vibration event
      $H_{S2} \leftarrow 0$
    else ▷start new vibration event
      $T \leftarrow 1/(f_s||\mathbf{v}||)$ ▷corresponding temporal period
      $H_{\mathrm{S2}}, T_a \leftarrow$ Algorithm 6 given T, A, j
      $j \leftarrow j + 1$ ▷increase vibration-event index
    end if
  else ▷ongoing vibration event
    $H_{\mathrm{S2}}, T_a \leftarrow$ Algorithm 6 given T_a, A, j
    $j \leftarrow j + 1$ ▷increase vibration-event index
    if $j = \mathrm{round}(\frac{T_a}{T_h})$ **then** ▷end of vibration event
      $j \leftarrow 0$ ▷reset vibration-event index
    end if
  end if
end procedure

IV. Human Subjects Experiments

This section describes three human-subject experiments that were conducted to quantitatively evaluate the methods described in Sections II and III by pairwise comparison. The study was approved by the University of Utah Institutional Review Board (IRB #00 096 461).

A. Experiment 1: T1 Vs. T3

This experiment was designed to compare temporal methods T1 and T3 in terms of both haptic and audio fidelity, across a range of frequencies and intensities. In this experiment, vibrations are displayed as subjects quasistatically touch a flat virtual surface.

1) Subjects: The study was performed by 12 (six male, six female) subjects, ages 19–30, who are student volunteers that gave informed consent. Two subjects (one male, one female) are left handed and the remaining subjects are right handed. All subjects had normal tactile sensation, normal auditory sensation, and normal (corrected) vision, by self-report.

2) Apparatus: We used the Phantom Omni (currently sold as 3D Systems Touch) haptic device in this study. This devices has a nominal position resolution of 0.055 mm in the workspace and a maximum exertable force of 3.3 N. It was controlled through CHAI3D [45] with a 1 kHz haptic update rate on a desktop computer running the Windows 10 operating system. We used a 483 mm (19 in) monitor with a 1280×1024 resolution to provide visual display with a 60 Hz refresh rate. The experimental setup is shown Fig. 7.

Forces were always generated in a single direction, which we chose to be vertical. It is well known that humans cannot distinguish the direction of high-frequency vibrations [8], and It has also been shown that the sensation associated with a given vibration intensity is largely invariant to the direction of a force-driven vibration [23], [42], [46]–[48]. We characterized the performance of our haptic device in the nominal configuration of our experiment; this is described in Appendix A.

3) Design: Experiment 1 uses a full-factorial repeated-measures design with three treatment factors: the temporal frequency f_t of the vibration, the intensity (i.e., amplitude A) of the vibration, and a binary auditory-feedback condition. We consider 12 temporal frequencies that can be uniquely

(a)

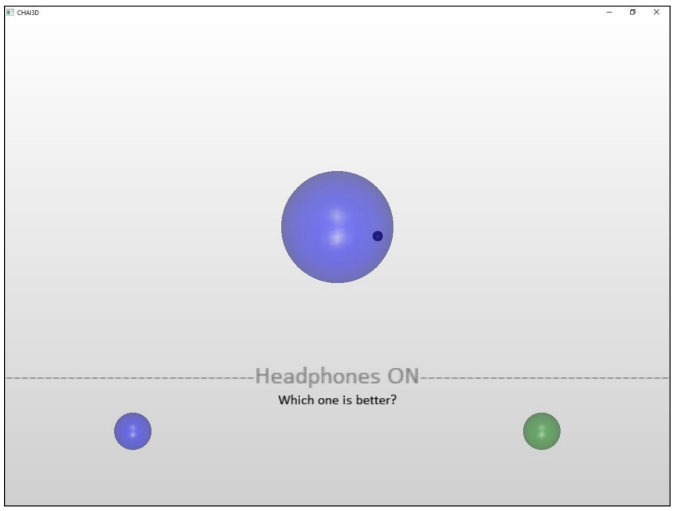

(b)

Fig. 7. Experimental setup. (a) The subject sits directly in front of a desktop monitor, holding the stylus of the Phantom Omni with a precision grasp, with her forearm resting on an armrest. The subject is shown with headphones on. (b) Screenshot of Experiments 1 and 2. The large sphere is shown colored blue, indicating that the first vibration of a 2-AFC trial is being presented. The two selection icons in the bottom corners are used to indicate a preference at the end of a trial.

displayed by Method T3 within the range of 43.1–500 Hz, which are the 11 temporal frequencies corresponding to odd-period vibration signals within this range, as well as $f_t = 400$ Hz (since this is handled as a special case in Method T3). We chose 43.1 Hz because at frequencies lower than this value vibrations displayed by Method T3 are within both the haptic and audio JND of their neighbors. We consider two levels of vibration intensity, low ($A = 1.05$ N) and high ($A = 2.10$ N), which were chosen as follows. The authors conducted a pilot test among themselves to determine the lowest intensity for which they believed any potential artifacts could be easily perceived, and this value was chosen for the high intensity; the low intensity was then chosen as half of the high intensity. We consider two conditions of auditory feedback for haptic perceptions: one is with auditory cues and the other is without auditory cues. Half of the subjects (three male, three female) were randomly assigned to perform the experiment first with headphones on (i.e., without auditory cues), followed by headphones off (i.e., with auditory cues), and the other half of the subjects performed the experiment in the reverse order. The above treatment levels yield 48 distinct combinations. Each of the combinations is repeated three times per subject, yielding 36 trials per combination across all 12 subjects.

Each trial resulted in a preference of Method T1 or Method T3. Statistical significance was analyzed by considering a binomial distribution, which states that the probability of m successes in n trials if the preferences are chosen by random chance ($p = 0.5$) is calculated as:

$$P = \binom{n}{m} p^m (1-p)^{n-m} = \frac{n!}{m!(n-m)!} p^m (1-p)^{n-m}. \quad (14)$$

We consider the cumulative probability of successes centered around $m = 18$ (i.e., exactly 50% successes) to determine the number of successes that should be deemed to be significantly different from $m = 18$, at some specified significance. Using a conventional significance of $\alpha = 0.05$, with 48 individual pairwise comparisons, the (conservative) Bonferroni correction suggests to use a significance of $\alpha^* = \alpha/48 \approx 0.001$ for each individual pairwise comparison. As a result, we concluded that there is significant preference for a method, for any particular combination, when the method is preferred at least 28 out of 36 trials for that combination. All analysis was done with MATLAB 2017b.

4) Procedure: The psychophysical experiment was conducted as a training session followed by a testing session. The training session lasted approximately 5 minutes and the testing session lasted 30–40 minutes per subject. At the beginning of the experiment, the subject sat in front of the table with the haptic device on it (see Fig. 7(a)), at a distance of approximately 0.7 m from the monitor; the subject was instructed to rest their forearm on the armrest and hold the stylus of the haptic device using a precision grasp (which was demonstrated to the subject). Before the experiment began, the subject was encouraged to adjust the height of the chair, the height of the armrest, and the position of the haptic device (including right or left handed) to facilitate a comfortable precision grasp on the stylus.

During the experiment, the subject used the stylus of the haptic device to control the cursor, which represented the position of HIP, in a 2D GUI displayed on the monitor (Fig. 7(b)). The GUI comprised a large sphere in the middle, a statement of the condition of auditory feedback (i.e., "Headphones ON" or "Headphones OFF"), and two selection icons that included a small blue sphere in the bottom-left corner and a small green sphere in the bottom-right corner. The subject was instructed to move the cursor to the large sphere in the middle to start a trial and then remain inside of the sphere until it disappeared, indicating that the trial was completed. Within a trial, the subject was presented with one of Method T1 and Method T3 (as detailed below) in random order while the large sphere was

blue, and then after a brief pause (in which the large sphere was gray) was presented with the other method while the large sphere was green. We used a two-alternative-forced-choice (2-AFC) procedure, forcing the subject to select which method they preferred, which was done by selecting the corresponding icon. If the subject accidentally moved the cursor out of the large sphere before a trial was complete, the trial was stopped and could be restarted from the beginning by moving the cursor back into the large sphere.

In a given trial, for a given method, the subject was presented with a progression of three distinct temporal vibrations—at low, medium, and high frequencies—where the medium frequency was one of the 12 f_t values described in Section IV-A3 and the low and high frequencies were the two neighboring frequencies (i.e., the one below and the one above) depicted in Fig. 3. Each vibration within a progression lasted 1 s, separated by a 0.5 s pause (i.e., no vibration). The two progressions (i.e., the two methods) were separated by a 1 s pause, with the change in color described earlier. Each trial forced the subject to choose which sample was the better progression from low frequency to high frequency.

In the testing session, the subject experienced four distinct pairings of high/low intensity with headphones on/off, with one trial at each of the 12 frequencies described above; we refer to this as a block. Within each block, the four pairings were randomly assigned, and then the 12 frequencies were randomly assigned within each pairing. Each subject was then presented sequentially with three such blocks. This block structure was implemented to mitigate effects of learning and fatigue on the results. The subject could take a break at any time throughout the experiment, as requested. At the end of the testing session, we asked the subject the open-ended question: "How did you feel about this experiment?"

Before the testing session, the subject was given a training session in two phases. During the first phase, the subject was guided through all potential vibration samples that they would experience during the testing session. The training session began with a progression at low intensity, which comprised three even-period vibrations at low ($f_t = 20$ Hz, $T = 0.050$ s), medium ($f_t = 33$ Hz, $T = 0.030$ s), and high ($f_t = 42$ Hz, $T = 0.024$ s) frequencies. These three values were chosen because they can be perfectly displayed using both methods, they are perceived as a clear progression from low to medium to high, and they would not be repeated in the testing session to avoid any potential learning effect. The subject was instructed to note the progression from low to medium to high. The progression was repeated at high intensity, and subjects were instructed to note that, although the vibrations felt stronger, there was still a progression from low to medium to high. The low- and high-intensity progressions were then repeated to enable the subject to feel them each again. The subject was told that what they had just felt was the type of progression that we were attempting to create throughout the study. The subject was then instructed that a progression is considered worse than the desired progression if any of three things happen: (1) the progression is not clearly from low to medium to high; (2) there are any noisy/gritty sensations; (3) there is a net force in one direction. These three cases were individually demonstrated to the subject, at low intensity, using the following three vibration signals, respectively, sandwiched between two even-period vibrations at the same low ($f_t = 20$ Hz, $T = 0.050$ s) and high ($f_t = 42$ Hz, $T = 0.024$ s) frequencies as the desired progression demonstrated above: (1) an even-period vibration at low (20 Hz) temporal frequency; (2) an odd-period vibration at $f_t = 34$ Hz ($T = 0.029$ s) displayed using Method T2, which the authors found to have particularly strong undesirable noisy/gritty artifacts in pilot testing; and (3) an even-period medium ($f_t = 33$ Hz, $T = 0.030$ s) vibration superimposed with a net force of 0.5 N upward. These three undesirable progressions were then repeated at high intensity. In this first phase of the training session, the word "Low," "Medium," or "High" was displayed on the monitor, as was "Low Intensity" or "High Intensity," corresponding to the haptic sensation being provided; such information was not provided to the subjects during the actual experiment.

For the second phase of the training session, the subject was exposed to the experimental protocol and the GUI of Fig. 7 (b). They performed six 2-AFC trials. We designed this phase using the six worst progression samples (i.e., those with the largest negative artifacts), including three at low intensity and three at high intensity, such that it would be easy for the subject to perceive the difference between the two choices and enter their selection.

5) Results: Fig. 8 shows the results of Experiment 1 for a significant preference for each of the 48 combinations. Method T1 is not preferred for any combination. Method T3 is preferred for 15 combinations: at high intensity, with or without auditory feedback, within the temporal frequency range of 111–400 Hz; at low intensity, with auditory feedback, within the temporal frequency range of 200–400 Hz; and at low intensity, without auditory feedback, within the temporal frequency range of 333–400 Hz.

The subjects' feedback that we collected at the end of the experiment, which is in agreement with the authors' perception, can be summarized as follows. A difference between the two samples in a trial was not noticeable for most of the trials. There was a net force combined with a smooth vibration for some trials. There is a net force combined with a noisy/gritty sensation for some trials. A net force is easier to detect at high intensity than at low intensity. Grasping the stylus more loosely made it easier to detect a net force.

6) Discussion: Fig. 2 shows how any odd-period vibration displayed by Method T1 causes a net force in one direction because the positive and negative impulses are not of equal magnitude. Method T3 takes this effect into account by generating asymmetric odd-period vibrations. Our experimental results suggest that this net-force effect is significantly noticeable and undesirable at high frequencies, and is further amplified by increasing the intensity of the vibrations. It is worth noting that the perceived net force due to asymmetric vibrations has been used as a desirable feature in a variety of ungrounded haptic displays [28]–[32].

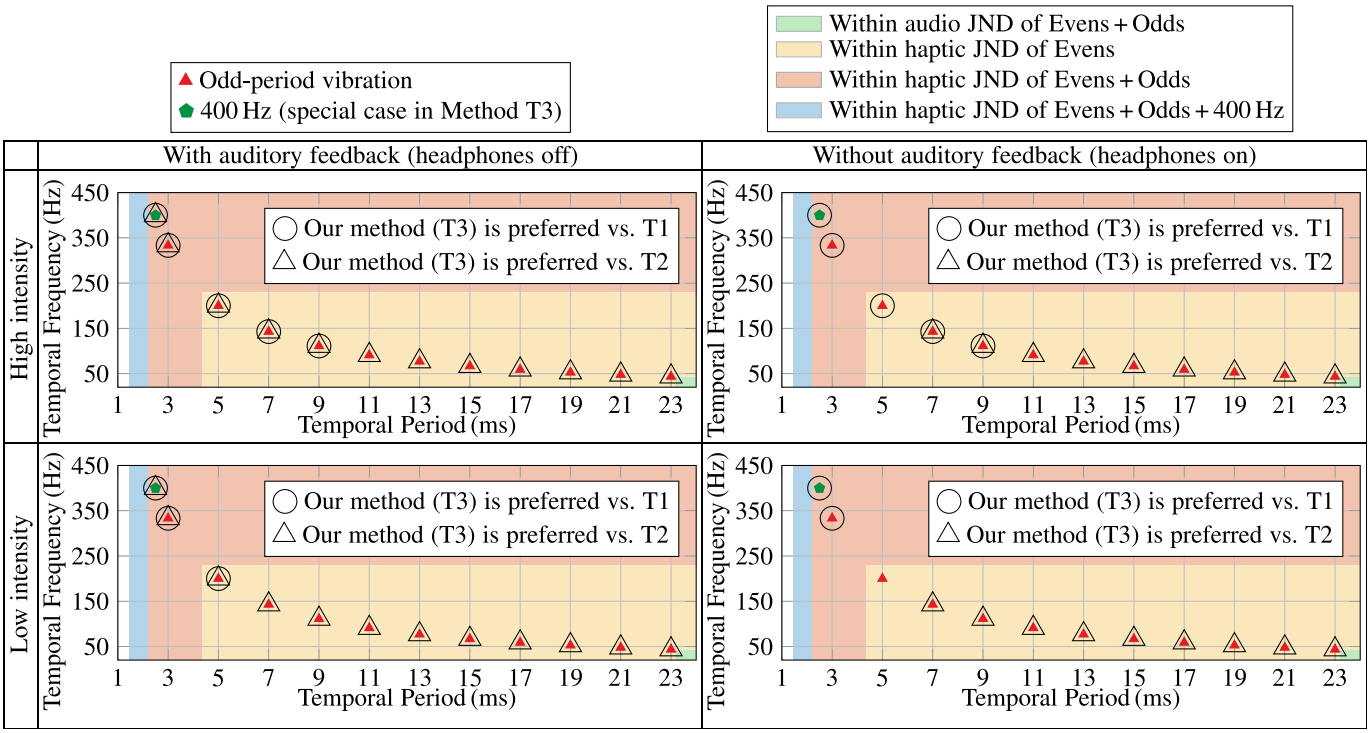

Fig. 8. Combined results of Experiments 1 and 2 for two levels of intensities (i.e., low and high), for two conditions of auditory feedback (i.e., headphones on and off), for 12 temporal frequencies within the range of 43.5–400 Hz corresponding to 11 odd-period vibrations as well as a vibration at a perceived frequency of 400 Hz. Symbols indicate when our proposed Method T3 is significantly preferred compared to Method T1 or T2. There was no evidence of a significant preference for Method T1 or T2 for any combination.

We found that subjects preferred Method T3 over Method T1 for displaying the temporal vibration at 400 Hz for both intensities and both conditions of auditory feedback. According to the authors' own perception, the 400 Hz vibration displayed by Method T1 has both a net force and a noisy/gritty sensation.

B. *Experiment 2: T2 Vs. T3*

This experiment was designed to compare temporal methods T2 and T3 in terms of both haptic and audio fidelity, across a range of frequencies and intensities. In this experiment, vibrations are displayed as subjects quasistatically touch a flat virtual surface. It is structured almost identically to Experiment 1.

1) Subjects: See Section IV-A1. In Experiment 2, six of the subjects, including both left-handed subjects, also participated in Experiment 1.

2) Apparatus: See Section IV-A2.

3) Design: See Section IV-A3. The only difference in Experiment 2 was that the two levels of vibration intensity were set to a low intensity of $A = 0.35$ N and a high intensity of $A = 0.7$ N. These are lower than the two intensity levels considered in Experiment 1 because the potential artifacts in this Experiment 2 are easier to detect, based on our pilot tests.

4) Procedure: See Section IV-A4.

5) Results: Fig. 8 shows the results of Experiment 2 for a significant preference for each of the 48 combinations. Method T2 is not preferred for any combinations. Method T3 is preferred for 42 combinations: at both high and low intensity, with auditory feedback, within the temporal frequency range of 43.5–400 Hz; and at both high and low intensity, without auditory feedback, within the temporal frequency range of 43.5–143 Hz.

The subjects' feedback that we collected at the end of the experiment, which is in agreement with the authors' perception, can be summarized as follows. The difference between the two samples in a trial was noticeable for most of the trials. There are noisy/gritty sensations for some trials. Grasping the stylus more loosely made it easier to detect the noisy/gritty sensations.

6) Discussion: We found that subjects preferred Method T3 over Method T2 at all frequencies tested when there was auditory feedback, but only at relatively low frequencies without audio feedback. That is, there is clearly a haptic benefit to Method T3 over Method T2 at relatively high frequencies, but Method T3 sounds better than Method T2 in cases in which they are haptically indistinguishable. In addition, these results are insensitive to the intensity of the vibration. These results are consistent with prior works that have shown that our ears are more sensitive in frequency discrimination than our hands, especially at high frequencies [41], [49].

The results at 400 Hz were consistent with the other high-frequency vibrations described above. Method T2 and Method T3 use the same basic mixing procedure for this temporal vibration, with the distinction being that Method T2 mixes 500 Hz with 250 Hz (the two neighboring even-period vibrations) whereas Method T3 mixes 500 Hz with 333 Hz (the two

closest neighbors considering both even-period and odd-period vibrations). According to the authors' own perception, the progression with 400 Hz vibration displayed by Method T3 sounds better than the same progression displayed by Method T2, in that the middle frequency sounds more like it is at the midpoint between the lower (333 Hz) and higher (500 Hz) frequencies in the progression. This suggests that the temporal frequencies of the individual vibration components used in the mixing procedure affect the perceived audio frequency of the mixed signal.

Although our experimental results found that our proposed temporal Method T3 is significantly preferred over Method T2 (which is an extension of [18]) for most cases that we considered, it must be noted that there are a number of differences between our experimental conditions and those of [18]. In fact, the method seems to work well in [18], leading to their conclusion that a haptic grating with multiple frequency components might be perceived as a single pitch; this is what motivated us to consider the method here. That work aims to render virtual haptic gratings with relative high spatial frequencies (≥ 1 mm^{-1}) using ultrasonic friction reduction on the haptic display. Subjects perceived vibrotactile feedback with their finger directly touching the haptic surface. Finally, they display sinusoidal signals at a update rate of 10 kHz.

C. Experiment 3: S1 Vs. S2

This experiment was designed to compare spatiotemporal methods S1 and S2 in the rendering of a 1D haptic gratings, across a range of spatial frequencies. In this experiment, vibrations are displayed as subjects actively scan across a haptic-grating virtual surface.

1) Subjects: See Section IV-A1. All subjects also participated in Experiment 1.

2) Apparatus: See Section IV-A2.

3) Design: Experiment 3 uses a design with one treatment factor: the spatial period λ of the virtual haptic square-wave grating. We consider three spatial periods of $\lambda = 0.5$ mm, $\lambda = 1$ mm, and $\lambda = 2$ mm (i.e., spatial frequencies of $f_s = 2$ mm^{-1}, $f_s = 1$ mm^{-1}, and $f_s = 0.5$ mm^{-1}, respectively). Each of the three spatial periods is displayed once per subject, which yields 12 trials across all subjects for each spatial period.

Each trial resulted in a preference of Method S1 or Method S2. Statistical significance was analyzed by considering the binomial distribution (14). We consider the cumulative probability of successes centered around $m = 6$ (i.e., exactly 50% successes) to determine the number of successes that should be deemed to be significantly different from $m = 6$, at some specified significance. Using a conventional significance of $\alpha = 0.05$, with three individual pairwise comparisons, the (conservative) Bonferroni correction suggests to use a significance of $\alpha^* = \alpha/3 \approx 0.017$ for each individual pairwise comparison. As a result, we concluded that there is significant preference for a method when the method is preferred at least 10 out of 12 trials for that specific spatial period. All analysis was done with MATLAB 2017b.

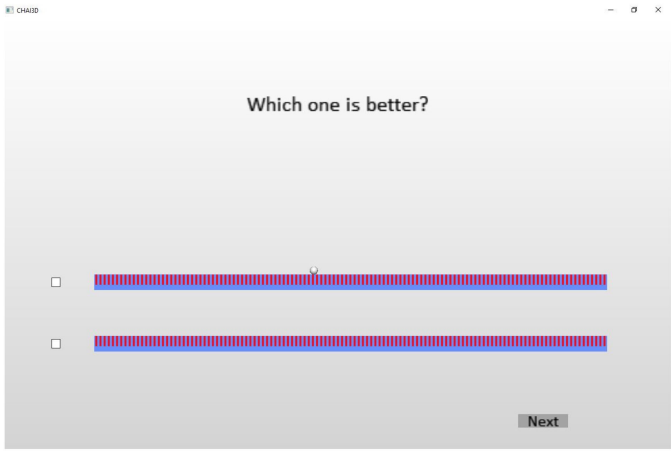

Fig. 9. Screenshot of Experiment 3. The spatial period of the two virtual surfaces shown is $\lambda = 2$ mm ($f_s = 0.5$ mm^{-1}).

4) Procedure: This psychophysical experiment lasted 5–15 minutes per subject. At the beginning of the experiment, the subject sat in front of the table with the haptic device on it (see Fig. 7(a)), at a distance of approximately 0.7 m from the monitor; the subject was instructed to rest their forearm on the armrest and hold the stylus of the haptic device using a precision grasp (which was demonstrated to the subject). Before the experiment began, the subject was encouraged to adjust the height of the chair, the height of the armrest, and the position of the haptic device (including right or left handed) to facilitate a comfortable precision grasp on the stylus.

During the experiment, the subject used the stylus of the haptic device to control the cursor, which represented the position of HIP, in a 2D GUI displayed on the monitor (Fig. 9). The GUI comprised two blue horizontal rectangles, rendered with a stiffness of $K = 0.7$ N/mm, which is well below the stability limit of the haptic device. On each of the top surfaces was rendered a haptic grating with a common spatial frequency and a common amplitude of $A = 2.7$ mm, one using Methods S1 and the other using Method S2, but visually identical. The grating was visually rendered with alternating red and blue thin vertical rectangles. The ordering of the methods was randomized for each subject. The other three sides of the rectangles were rendered as smooth frictionless surfaces. A proxy was used such that the cursor did not penetrate the surface of the virtual objects. The subject was instructed to move the cursor to freely explore both haptic gratings for at least one minute per trial, and was encouraged to try various scanning speeds. The GUI also posed the question "Which one is better?," and included check boxes that could be clicked to indicate a selection. We used a 2-AFC procedure, forcing the subject to select which surface they thought felt better. The subject was provided no information regarding the rendering methods, and they were given no directions regarding what "better" meant. The subject completed three such trials, one for each of the spatial frequencies, presented in a random order. The subject could take a break at any time throughout the experiment, as requested.

5) Results: For the spatial period of $\lambda = 0.5$ mm, a preference for Method S2 over Method S1 was found in 12 out of 12 trials (i.e., 12 out of 12 subjects), which is significant. For $\lambda = 1$ mm, a preference for Method S2 was found in 11 out of 12 trials, which is also significant. For $\lambda = 2$ mm, a preference for Method S2 was found in only 7 out of 12 trials, which is not significant.

6) Discussion: Prior studies [6], [44] suggested that common scanning speeds used in haptic textures display are in the range of 0–250 mm/s. Using these values, our three spatial periods of $\lambda = 0.5$ mm, $\lambda = 1$ mm, and $\lambda = 2$ mm would correspond to temporal frequencies as high as $f_t = 500$ Hz, $f_t = 250$ Hz, and $f_t = 125$ Hz, respectively. If we consider the results of Experiment 1 with audio feedback and at low intensity, which are the most analogous to Experiment 3, we find that Method T3 (i.e., the temporal version Method S2) was superior to Method T1 (i.e., the temporal version of Method S1) for temporal frequencies at or above $f_t = 200$ Hz, but the same could not be said of lower frequencies. Those results seem consistent with the results of Experiment 3, in light of [6], [44].

In Method S2, we chose to implement a scanning-speed deadband at 1 mm/s (see Alg. 7, line 3) based on pilot testing, and this is the value that we used in Experiment 3. In practice, we found that implementing some deadband resulted in a better feel than no deadband, but the value of 1 mm/s could likely be changed slightly without significantly affecting the results (and others may prefer a slightly different value).

Our results for Method S1 are not particularly surprising, considering that Choi and Tan [10], [43] noted that haptic display of sinusoidal gratings using an update rate lower than 10 kHz when reconstructing the corresponding height map using ZOH (i.e., Method S1) might cause "buzzing" due to signal aliasing. Since humans cannot distinguish square-wave gratings and sinusoidal gratings based on their waveform [22], these perceived artifacts would likely also occur in haptic display of square-wave gratings. However, in our perception, the problem with Method S1 is better described as "dropout" than "buzzing," since the aliasing can cause a complete lack of high-frequency sensation at certain scanning velocities.

V. Discussion

For the display of open-loop temporal vibrations, the results of Experiments 1 and 2 indicate that subjects either prefer our proposed method (Method T3), or cannot distinguish methods, across the entire frequency range of 20–500 Hz tested. In a subsequent study involving the authors, we displayed a continuous sweep through the full frequency range and found that Method T1 sounded continuous, whereas we could hear discontinuities in Method T3. This solidified our opinion that the preference for Method T3 over Method T1 was clearly due to haptic effects (i.e., the net force).

To enable vibrotactile display over the entire frequency range of 20–1000 Hz that humans are able to detect, the success of Method T3 seems to suggest that a haptic update rate of 2 kHz would be sufficient to render the entire range; this is well below the previous suggested requirements of 5–10 kHz [10]. With an update rate of 2 kHz, we would be capable of displaying even-period and odd-period temporal vibrations at 1000 Hz, 667 Hz, 500 Hz, and 400 Hz, and then displaying 800 Hz by mixing 1000 Hz and 667 Hz using a method analogous to Algorithm 5. These values would be sufficient to ensure that all displayable frequencies are within the haptic JND of their neighbors.

Since the highest temporal frequency that can be generated by a haptic device running with a 1 kHz update rate is $f_t = 500$ Hz, the 250 mm/s maximum scanning speed suggested by [6] would seem to suggest that the smallest haptic-grating spatial period that we should expect to render with high fidelity is $\lambda = 0.5$ mm (i.e., $f_s = 2$ mm^{-1}). However, if we also consider the haptic JND of $+190$ Hz at $f_t = 500$ Hz, based on a Weber fraction of approximately 0.38 from [34], we conclude that the actual smallest haptic-grating spatial period that we should expect to render with high fidelity using our proposed method is $\lambda = 0.36$ mm (i.e., $f_s = 2.8$ mm^{-1}).

Experiment 3 indicates that subjects prefer our spatiotemporal Method S2 over Method S1 (which is described in [5]) for the display of haptic gratings with relatively high spatial frequency. However, a drawback with Method S2 is that graphical and haptic information are not necessarily perfectly synchronized, which is not the case with Method S1. The results of Experiment 3 may seem to suggest that the two methods are indistinguishable for the haptic grating with relatively low spatial frequency ($\lambda \leq 2$ mm), but we actually believe that Method S1 is superior for low spatial frequency for the reason described above.

VI. Conclusion

In this paper, we proposed a method to display vibrotactile stimulus signals of moderate to high frequency (20–500 Hz) using kinesthetic haptic devices with a standard 1 kHz haptic update rate. Our method combines symmetric square-wave signals whose periods are even multiples of the haptic update period with asymmetric square-wave signals whose periods are odd multiples of the haptic update period, while ensuring that the positive and negative impulses are balanced in both cases, and utilizing the just noticeable difference in frequency discrimination to avoid the need to display other frequencies. For frequencies at which this balanced-impulse method is insufficient, corresponding to a small band near 400 Hz for a 1 kHz update rate, we utilize a modification of a prior signal-mixing method. Our complete method was then extended to render haptic gratings by measuring scanning velocity, converting the local spatial frequency to its equivalent temporal frequency, and displaying a single full-period vibration event. In a series of human-subject studies considering both haptic and audio quality, we showed that our proposed method is preferred over existing methods for vibrotactile display of signals with relatively high-frequency content.

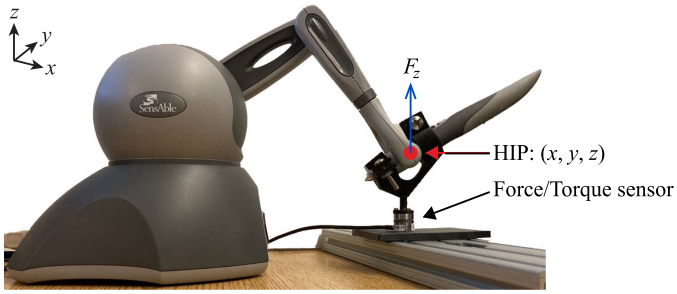

Fig. 10. Experimental setup for characterizing the force output of Phantom Omni. The stylus of Phantom Omni is rigidly connected to the force/torque sensor using a 3D-printed fixture.

the frequencies that we used in the human-subjects experiments). We commanded force signals with a square-wave amplitude of $A = 1$ N. We gathered data for four runs at 10 s of data per run. For each run, we gather 1 s of data before and after each run, which we average to subtract off any bias in the force measurements.

In our characterization of the Phantom Omni, we repeated the steps of Section II-D to get the experimental results shown in Fig. 11. Although imperfections in the Phantom Omni make the experimental results differ from those of the idealized signals in Fig. 4, the important features are largely maintained. The fundamental components

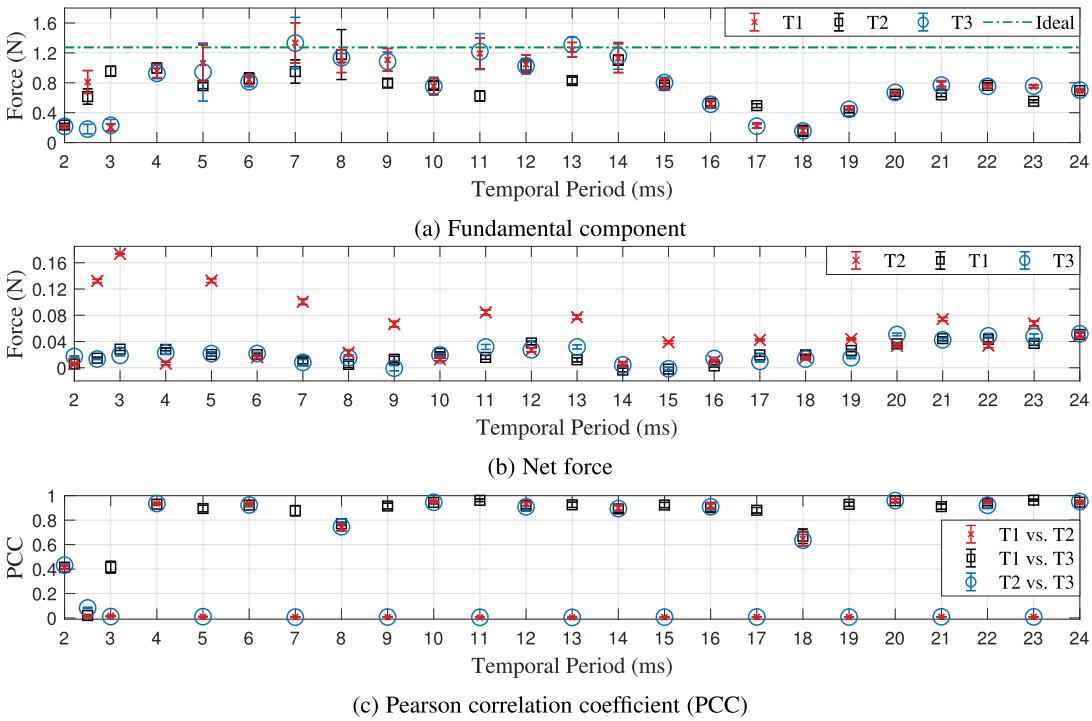

Fig. 11. Experimental results characterizing the force output of the Phantom Omni. The measured force signals are rendered using each of the three candidate temporal methods, across temporal periods T in the range 0.002–0.024 s, corresponding to a desired intensity of $A = 1$ N, which has an ideal fundamental component of 1.27 N, and a desired net force of 0 N. All signals are rendered at 1 kHz, and force measurements are taken at 40 kHz. The measured values are depicted as means with 95% confidence intervals based on four 10-s data sets. (a) Fundamental component. (b) Net force, (c) Pearson correlation coefficient (PCC).

APPENDIX A
CHARACTERIZING THE PHANTOM OMNI

We performed experiments to characterize the performance of the Phantom Omni using an ATI Nano17 six-axis force/torque sensor with a National Instruments PCIe 6320 data-acquisition card with a 40 kHz sampling rate. We fabricated a custom fixture that rigidly fixed the HIP of the device directly above the sensor, with the device in the nominal configuration used during the human-subject studies (Fig. 10). We commanded vertical forces (as in our human-subject experiments) using the three candidate temporal methods (i.e., Method T1–T3) to display the desired square-wave vibrations with even-period, odd-period, and 400 Hz throughout the frequency range of 42–500 Hz (i.e., over

and PCC values indicate that the perceived amplitude and overall frequency content is the same across most frequencies for Methods T1 and T3, as well as for Method T2 for even-period signals. We also see the substantial parasitic net force of Method T1 at relatively high frequencies (i.e., relatively small temporal periods), although we actually observe a small net force for all three methods at nearly all frequencies tested. There are three major differences between the experimental results and the idealized signals. First, the amplitude of the fundamental component of the measured signals is often well below the desired value. However, since this effect seems to affect Methods T1 and T3 equally, there is no reason to believe it will impact the human-subjects experiment comparing T1 and T3. Second, at the highest frequencies (i.e., temporal periods of 2 ms

and 3 ms), the PCC indicates differences between Methods T1 and T3 that were not anticipated, whereas we did not observe the small differences in the amplitude of the fundamental components that were anticipated. It seems that the dynamics of the haptic device are affecting the output force signal, causing the differences between Methods T1 and T3 to manifest themselves differently than anticipated. Third, the amplitude of the fundamental components of the odd-period signals with Method T2 are much larger than anticipated. It is possible that the inertia of the haptic device is serving to low-pass filter the T2 signals, which tend to have higher-frequency content that the respective signals with T1 and T3. The effect of this discrepancy is the possibility that Method T2 will feel more similar to Methods T1 and T3 than anticipated.

ACKNOWLEDGMENT

The authors would like to thank Lan N. Pham for technical assistance in our pilot study. They would also like to thank Dr. John Hollerbach and the anonymous reviewers for their suggestions.

REFERENCES

[1] H. Culbertson, S. B. Schorr, and A. M. Okamura, "Haptics: The present and future of artificial touch sensation," *Annu. Rev. Control, Robot., Auton. Syst.*, vol. 1, pp. 385–409, 2018.

[2] A. M. Okamura, M. R. Cutkosky, and J. T. Dennerlein, "Reality-based models for vibration feedback in virtual environments," *IEEE/ASME Trans. Mechatronics*, vol. 6, no. 3, pp. 245–252, Sep. 2001.

[3] K. J. Kuchenbecker, J. Fiene, and G. Niemeyer, "Improving contact realism through event-based haptic feedback," *IEEE Trans. Vis. Comput. Graph.*, vol. 12, no. 2, pp. 219–230, Mar.–Apr. 2006.

[4] S. Choi and H. Z. Tan, "Toward realistic haptic rendering of surface textures," *IEEE Comput. Graph. Appl.*, vol. 24, no. 2, pp. 40–47, Mar.–Apr. 2004.

[5] S. A. Cholewiak, K. Kim, H. Z. Tan, and B. D. Adelstein, "A frequency-domain analysis of haptic gratings," *IEEE Trans. Haptics*, vol. 3, no. 1, pp. 3–14, Jan.–Mar. 2010.

[6] H. Culbertson, J. Unwin, and K. J. Kuchenbecker, "Modeling and rendering realistic textures from unconstrained tool-surface interactions," *IEEE Trans. Haptics*, vol. 7, no. 3, pp. 381–393, Jul.–Sep. 2014.

[7] S. Papetti and C. Saitis, Eds. *Musical Haptics*. Springer Open, 2018.

[8] J. Bell, S. Bolanowski, and M. H. Holmes, "The structure and function of pacinian corpuscles: A review," *Prog. Neurobiol.*, vol. 42, no. 1, pp. 79–128, 1994.

[9] S. Bensmaïa, M. Hollins, and J. Yau, "Vibrotactile intensity and frequency information in the pacinian system: A psychophysical model," *Perception Psychophysics*, vol. 67, no. 5, pp. 828–841, 2005.

[10] S. Choi and H. Z. Tan, "Perceived instability of virtual haptic texture: III. effect of update rate," *Presence: Teleoperators Virtual Environ.*, vol. 16, no. 3, pp. 263–278, 2007.

[11] A. El Saddik, M. Orozco, M. Eid, and J. Cha, *Haptics Technologies: Bringing Touch to Multimedia*. Berlin, Germany: Springer-Verlag, 2011.

[12] S. Choi and K. J. Kuchenbecker, "Vibrotactile display: Perception, technology, and applications," *Proc. IEEE*, vol. 101, no. 9, pp. 2093–2104, Sep. 2013.

[13] G. Campion and V. Hayward, "Fundamental limits in the rendering of virtual haptic textures," in *Proc. IEEE World Haptics Conf.*, 2005, pp. 263–270.

[14] H. Culbertson, J. J. L. Delgado, and K. J. Kuchenbecker, "One hundred data-driven haptic texture models and open-source methods for rendering on 3D objects," in *Proc. IEEE Haptics Symp.*, 2014, pp. 319–325.

[15] S. Shin and S. Choi, "Geometry-based haptic texture modeling and rendering using photometric stereo," in *Proc. IEEE Haptics Symp.*, 2018, pp. 262–269.

[16] M. B. Kocsis, S. A. Cholewiak, R. M. Traylor, B. D. Adelstein, E. D. Hirleman, and H. Z. Tan, "Discrimination of real and virtual surfaces with sinusoidal and triangular gratings using the fingertip and stylus," *IEEE Trans. Haptics*, vol. 6, no. 2, pp. 181–192, Apr.–Jun. 2013.

[17] D. J. Meyer, M. A. Peshkin, and J. E. Colgate, "Modeling and synthesis of tactile texture with spatial spectrograms for display on variable friction surfaces," in *Proc. IEEE World Haptics Conf.*, 2015, pp. 125–130.

[18] R. F. Friesen, R. L. Klatzky, M. A. Peshkin, and J. E. Colgate, "Single pitch perception of multi-frequency textures," in *Proc. IEEE Haptics Symp.*, 2018, pp. 290–295.

[19] F. W. Campbell and J. Robson, "Application of fourier analysis to the visibility of gratings," *J. Physiol.*, vol. 197, no. 3, pp. 551–566, 1968.

[20] H. T. Nefs, A. M. Kappers, and J. J. Koenderink, "Amplitude and spatial-period discrimination in sinusoidal gratings by dynamic touch," *Perception*, vol. 30, no. 10, pp. 1263–1274, 2001.

[21] H. T. Nefs, A. M. Kappers, and J. J. Koenderink, "Detection of amplitude modulation and frequency modulation in tactual gratings: A critical bandwidth for active touch," *Perception*, vol. 32, no. 10, pp. 1259–1271, 2003.

[22] I. R. Summers, P. G. Cooper, P. Wright, D. A. Gratton, P. Milnes, and B. H. Brown, "Information from time-varying vibrotactile stimuli," *J. Acoust. Soc. Amer.*, vol. 102, no. 6, pp. 3686–3696, 1997.

[23] N. Landin, J. M. Romano, W. McMahan, and K. J. Kuchenbecker, "Dimensional reduction of high-frequency accelerations for haptic rendering," in *Proc. Int. Conf. Hum. Haptic Sens. Touch Enabled Comput. Appl.*, 2010, pp. 79–86.

[24] J. C. Makous, R. M. Friedman, and C. J. Vierck, "A critical band filter in touch," *J. Neurosci.*, vol. 15, no. 4, pp. 2808–2818, 1995.

[25] G. Park and S. Choi, "Perceptual space of amplitude-modulated vibrotactile stimuli," in *Proc. IEEE World Haptics Conf.*, 2011, pp. 59–64.

[26] SC. Lim, KU.Kyung, and D.S.Kwon, "Effect of frequency difference on sensitivity of beats perception," *Exp. Brain Res.*, vol. 216, no. 1, pp. 11–19, 2012.

[27] I. Hwang, J. Seo, and S. Choi, "Perceptual space of superimposed dual-frequency vibrations in the hands," *PLoS One*, vol. 12, no. 1, 2017, Art. no. e0169570.

[28] J.-P. Choiniere and C. Gosselin, "Development and experimental validation of a haptic compass based on asymmetric torque stimuli," *IEEE Trans. Haptics*, vol. 10, no. 1, pp. 29–39, Jan.–Mar. 2017.

[29] H. Culbertson, J. M. Walker, and A. M. Okamura, "Modeling and design of asymmetric vibrations to induce ungrounded pulling sensation through asymmetric skin displacement," in *Proc. IEEE Haptics Symp.*, 2016, pp. 27–33.

[30] H. Culbertson, J. M. Walker, M. Raitor, and A. M. Okamura, "Waves: A wearable asymmetric vibration excitation system for presenting three-dimensional translation and rotation cues," in *Proc. CHI Conf. Hum. Factors Comput. Syst*. ACM, 2017, pp. 4972–4982.

[31] T. Tanabe, H. Yano, and H. Iwata, "Evaluation of the perceptual characteristics of a force induced by asymmetric vibrations," *IEEE Trans. Haptics*, vol. 11, no. 2, pp. 220–231, Apr.–Jun. 2018.

[32] H. W. Tappeiner, R. L. Klatzky, B. Unger, and R. Hollis, "Good vibrations: Asymmetric vibrations for directional haptic cues," in *Proc. IEEE World Haptics Conf.*, 2009, pp. 285–289.

[33] G. D. Goff, "Differential discrimination of frequency of cutaneous mechanical vibration." *J. Exp. Psychol.*, vol. 74, no. 2p1, pp. 294–299, 1967.

[34] A. Israr, H. Z. Tan, and C. M. Reed, "Frequency and amplitude discrimination along the kinesthetic-cutaneous continuum in the presence of masking stimuli," *J. Acoust. Soc. Amer.*, vol. 120, no. 5, pp. 2789–2800, 2006.

[35] G. W. Young, D. Murphy, and J. Weeter, "Haptics in music: The effects of vibrotactile stimulus in low frequency auditory difference detection tasks," *IEEE Trans. Haptics*, vol. 10, no. 1, pp. 135–139, Jan.-Mar. 2017.

[36] O. Franzén and J. Nordmark, "Vibrotactile frequency discrimination," *Perception Psychophysics*, vol. 17, no. 5, pp. 480–484, 1975.

[37] M. Rothenberg, R. T. Verrillo, S. A. Zahorian, M. L. Brachman, and S. J. Bolanowski Jr, "Vibrotactile frequency for encoding a speech parameter," *J. Acoust. Soc. Amer.*, vol. 62, no. 4, pp. 1003–1012, 1977.

[38] K. Horch, "Coding of vibrotactile stimulus frequency by pacinian corpuscle afferents," *J. Acoust. Soc. Amer.*, vol. 89, no. 6, pp. 2827–2836, 1991.

[39] A. K. Goble and M. Hollins, "Vibrotactile adaptation enhances frequency discrimination," *J. Acoust. Soc. Amer.*, vol. 96, no. 2, pp. 771–780, 1994.
[40] M. A. Rinker, J. C. Craig, and L. E. Bernstein, "Amplitude and period discrimination of haptic stimuli," *J. Acoust. Soc. Amer.*, vol. 104, no. 1, pp. 453–463, 1998.
[41] G. A. Gescheider, *Psychophysics: The Fundamentals*. Psychology Press, Mahwah, NJ, 2013.
[42] G. Park and K. J. Kuchenbecker, "Objective and subjective assessment of algorithms for reducing three-axis vibrations to one-axis vibrations," in *Proc. IEEE World Haptics Conf.*, 2019, pp. 467–472.
[43] S. Choi and H. Z. Tan, "Perceived instability of virtual haptic texture. i. experimental studies," *Presence Teleoperators Virtual Environ.*, vol. 13, no. 4, pp. 395–415, 2004.
[44] H. Culbertson and K. J. Kuchenbecker, "Should haptic texture vibrations respond to user force and speed?," in *Proc. IEEE World Haptics Conf.*, 2015, pp. 106–112.
[45] F. Conti *et al.*, "The chai libraries," in *Proc. Eurohaptics*, 2003, pp. 496–500.
[46] A. Brisben, S. Hsiao, and K. Johnson, "Detection of vibration transmitted through an object grasped in the hand," *J. Neuriophysiol.*, vol. 81, no. 4, pp. 1548–1558, 1999.
[47] R. Zhang, A. J. Boyles, and J. J. Abbott, "Six principal modes of vibrotactile display via stylus," in *Proc. IEEE Haptics Symp.*, 2018, pp. 313–318.
[48] R. Zhang, T. J. Schwer, and J. J. Abbott, "Dimensional reduction for 6D vibrotactile display," *IEEE Trans. Haptics*, vol. 13, no. 1, pp. 102–108, Jan.–Mar. 2020.
[49] J. M. Yau, J. B. Olenczak, J. F. Dammann, and S. J. Bensmaia, "Temporal frequency channels are linked across audition and touch," *Curr. Biol.*, vol. 19, no. 7, pp. 561–566, 2009.

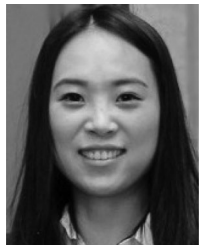

Ruisi Zhang (Student Member, IEEE) received the B.S. and M.S. degrees from Iowa State University, Ames, IA, USA, in 2012 and 2013, respectively, and is currently working toward the Ph.D. degree (Robotics Track) with the University of Utah, Salt Lake City, UT, USA, all in mechanical engineering. After graduation, she was a Research Intern with the Institute of Computing Technology, Chinese Academy of Sciences, Beijing, China. Her research interests include vibrotactile display with stylus-based kinesthetic haptic interfaces, including magnetic haptic interfaces.

Jake J. Abbott (Senior Member, IEEE) received the B.S. degree from the Utah State University, Logan, UT, USA, in 1999, the M.S. degree from the University of Utah, Salt Lake City, UT, USA, in 2001, and the Ph.D. degree from the Johns Hopkins University, Baltimore, MD, USA, in 2006, all in mechanical engineering. In 2006, he became a Postdoctoral Researcher with ETH Zurich, Zürich, Switzerland. In 2008, he joined the Department of Mechanical Engineering, University of Utah, where he is currently a Professor and core Member of the Robotics Center.